Experimental methodology to assess the dynamic equivalent stiffness properties of elliptical orthotropic plates

Fabien Marchetti, N.B. Roozen, Joost Segers, Kerem Ege, Mathias Kersemans, Quentin Leclere

Experimental methodology to assess the dynamic equivalent stiffness properties of elliptical orthotropic plates

Fabien Marchetti *

Matelys - Research Lab, F-69120 Vaulx-en-Velin, France

N.B. Roozen

KU Leuven, Laboratory of Acoustics, Department of Physics and Astronomy, Celestijnenlaan 200D, B-3001 Heverlee, Belgium

Joost Segers

Ghent Univ, Mechanics of Materials and Structures, Technologiepark 46, B-9052 Zwijnaarde, Belgium

Kerem Ege

Univ Lyon, INSA-Lyon, LVA EA677, F-69621 Villeurbanne, France

Mathias Kersemans

Ghent Univ, Mechanics of Materials and Structures, Technologiepark 46, B-9052 Zwijnaarde, Belgium

Quentin Leclère

Univ Lyon, INSA-Lyon, LVA EA677, F-69621 Villeurbanne, France

Abstract

This paper deals with the dynamic characterisation of plate structures with elliptical orthotropic stiffness properties, using an equivalent thin plate theory using a wave fitting approach. The method consists in projecting the experimentally determined transverse displacement field of a plate on an analytical Green's function of an elliptical orthotropic plate based on Hankel's functions. The error between the projected and measured fields is then minimized, varying the characteristics of the function until an optimal fit is reached. The thus obtained characteristics are the two flexural rigidities defining the elliptical orthotropy of the plate, and the orthotropy angle. This fitting procedure is applied at each

frequency, enabling the determination of frequency dependent dynamic material properties. The method is applied to a honeycomb sandwich panel to validate the proposed fitting approach. The identified flexural rigidities are compared to the estimations obtained by means of an analytical model and the IWC (Inhomogeneous Wave Correlation) method assuming three different type of plate characteristics (anisotropic, orthotropic and elliptical orthotropic). For the elliptical orthotropic assumption, consistent results are observed between the methods and the model over a large frequency range (from 1 to 50 kHz).

Key words: Elliptical orthotropy; sandwich panels; wave fitting approach; flexural rigidities; dynamic equivalent properties; experimental validation

1 Introduction

Nowadays, composite materials and honeycomb sandwich structures are widely used in industry. Different experimental procedures exist for the characterisation of such anisotropic structures. At high frequencies, where modal analysis approaches become inappropriate, other techniques based on vibration field analysis have demonstrated their efficiency. They can be classified in two main categories.

The first category comprises the global methods which consider the measurement data over a whole plate area. Among them, wave fitting approaches, such as the IWC (Inhomogeneous Wave Correlation) method developed by Berthaut et al. [1], stand out. The fitting methodology consists in correlating the measured vibration field with a numerically generated vibration field, consisting of plane waves, to identify the dispersion properties of the structure. The IWC method has been used in many applications. Cherif et al. [2] employed such an approach to characterize composite plates and aluminium panels treated with viscoelastic patches. Ichchou et al. [3] applied the IWC method assuming that the measured structure can be represented by a thin plate under Love-Kirchhoff's theory. They used this assumption to identify the dynamic flexural properties of a honeycomb sandwich plate. Finally, Rak et al. [4] showed that the IWC method gives different estimations of the structural loss factor as compared to McDaniel's method [5]. Another wave fitting approach has been developed by Cuenca et al. [6,7]. In this method, the projected field corresponds to the Green's function of a finite plate with simply supported

* corresponding author
Email addresses: fabien.marchetti@matelys.com (Fabien Marchetti), bert.roozen@kuleuven.be (N.B. Roozen), Joost.Segers@UGent.be (Joost Segers), kerem.ege@insa-lyon.fr (Kerem Ege), Mathias.Kersemans@UGent.be (Mathias Kersemans), quentin.leclere@insa-lyon.fr (Quentin Leclère).

boundary conditions and is constructed combining Hankel's functions and the image sources method. This fitting approach requires knowledge about the position of the source. As mentioned by Roozen et al. [8], the Green's function is *"better suited to represent the vibrational field of a point excited plate"*, especially close to the source and at high frequencies, as compared to the plane wave of the IWC method. The Hankel's functions are defined assuming that the measured structure behaves as a thin plate of Love-Kirchhoff. Based upon this assumption, the material properties identified by the method correspond to the complex flexural rigidity of the thin plate. Roozen et al. [8] proposed to combine the image source method with a bayesian regularisation to increase the accuracy of the method.

The second category of vibration field analysis methods comprises local approaches which locally solve the equation of motion of the structure. The main advantage of the local aspect is to apply the method without any knowledge outside the studied area (boundary conditions or sources). The FAT (Force Analysis Technique) approach [9] estimates the equation of motion by means of a finite different scheme applied on the measured vibration field. The bias error of this scheme is reduced with the CFAT (Corrected FAT) [10] approach by adding correction factors. The FAT and CFAT methods have been used to characterise isotropic [11,12] and orthotropic [13] plates modelling the measured structures as Love-Kirchhoff's thin plates. Another local approach is the VFM (Virtual Field Method) [14], which is based on the principle of virtual works. With this principle, the equation of motion is solved estimating the partial derivatives of the measured displacement field at the order 2 only. Hence, the VFM has the advantage to be less sensitive to measurement uncertainties than the FAT or CFAT methods.

In this paper, the Hankel fitting approach is adapted for the characterisation of plate structures defined by an elliptical orthotropic behaviour of the flexural motion, using the equivalent thin plate theory [15]. Spruce woods or honeycomb sandwich panels are good examples of such structures. The theory of the proposed method is detailed in Section 2. Then, Section 3 describes the IWC method and an analytical model, which will be used to validate the proposed Hankel fitting approach. Finally, an experimental application performed on a honeycomb sandwich plate is presented in Section 4.

2 Proposed method: Elliptical orthotropic Hankel fitting approach

This section details the adaptation of the Hankel fitting approach [6,8] for elliptical orthotropic plates. This type of plate is characterised by an elliptical wavenumber curve for flexural motion (see Figure 1). The method considers the transverse displacement field W of an harmonically excited plate measured over a regular grid mesh (x_p, y_q). An off-axes orthotropy is considered assuming that the main axes of the measurement mesh (x, y) are different from the orthotropy axes (x', y') of

the plate, as indicated in Figure 1. The angle between the two coordinate systems corresponds to the orthotropy angle θ'. The main idea of the methodology consists in approximating the measured displacement field by means of Green's functions of an elliptical orthotropic plate under Love-Kirchhoff's theory. The identification of the analytical expression of such functions for elliptical orthotropic plates is addressed in section 2.1. The fitting approach is then developed in section 2.2.

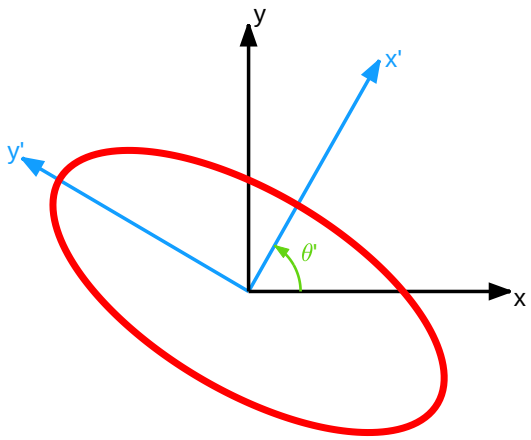

Fig. 1. Theoretical example of the flexural wavenumber curve of an elliptical orthotropic plate (red line). Axes of the measurement mesh (x, y). Orthotropy axes (x', y').

2.1 Elliptical orthotropic Green's function

The equation of motion of an elliptical orthotropic plate excited by a point force δ is defined in the (x', y') coordinate system by the Love-Kirchhoff's theory as:

$$\left(\left(\sqrt{D'_{11}}\frac{\partial^2}{\partial x'^2} + \sqrt{D'_{22}}\frac{\partial^2}{\partial y'^2}\right)^2 - \rho h\omega^2\right) w(x', y') = \delta(x' - x'_0, y' - y'_0), \quad (1)$$

where w is the transverse motion, ω is the angular frequency, ρ is the plate density, h is the plate thickness and (x'_0, y'_0) is the position of the source. The D' coefficients correspond to the flexural rigidities of the structure in the (x', y') coordinate system along the directions of orthotropy (see Figure 1).

For infinite lateral dimensions of the plate, the solution of Eq. (1) corresponds to an elliptical orthotropic Green's function G_∞. Berthaut [16] gave, in the appendix

of his thesis, the analytical expression [1] of such a function referring to Hamet [17]:

$$G_\infty(x', y', \omega) = \frac{\mathrm{j}\sqrt[4]{D'_{11}D'_{22}}}{8\sqrt{\rho h \omega^2}}\Big(H_0^{(1)}(\kappa r) - H_0^{(1)}(\mathrm{j}\kappa r)\Big), \tag{2}$$

where $H_0^{(1)}$ corresponds to the cylindrical Hankel's function of the first kind of order 0, κ is a pseudo-wavenumber and r is the source distance. The product between κ and r is defined by:

$$\kappa r = \sqrt[4]{\rho h \omega^2}\sqrt{\frac{(x'-x'_0)^2}{\sqrt{D'_{11}}} + \frac{(y'-y'_0)^2}{\sqrt{D'_{22}}}}. \tag{3}$$

Then, the Green's function (2) can be written in the (x, y) measurement coordinate system using the matrix relation (see Figure 1):

$$\begin{pmatrix} x' \\ y' \end{pmatrix} = \begin{bmatrix} \cos(\theta') & \sin(\theta') \\ -\sin(\theta') & \cos(\theta') \end{bmatrix} \begin{pmatrix} x \\ y \end{pmatrix}. \tag{4}$$

2.2 Fitting methodology

In [6,8], the image source method is used to account for the reflection of waves caused by the finiteness of the plate in lateral dimensions. The implementation of the image source method to orthotropic panels with arbitrary orthotropy angle is not straightforward. For such structures, a plane wave travelling to the edge with some angle is reflected in another direction with a different wavelength. Symmetrical Green's functions are used in the image source method to estimate the reflected field involving that the wavelength of the reflected wave remains the same as the incident wave. Thus, the validity of the image source method may be doubted for orthotropic panels with arbitrary orthotropy angle. The reader may notice that the method is yet valid if the orthotropy axes are aligned with the edges of the plate. Since the characterisation technique developed in this work can be applied on elliptical orthotropic plates with arbitrary orthotropy angle, we preferred not to use the image source method and neglect the reflected waves in the projected field. Based upon this assumption, the measured vibration field $W(x_p, y_q, \omega)$ can be approximated by the projected field:

$$\tilde{W}(x_p, y_q, \omega) = \alpha(\omega) G_\infty(x_p, y_q, \omega), \tag{5}$$

[1] Berthaut also tried different methods to identify the Green's function of non-elliptical orthotropic plates. He concluded that *"it is very sensitive or even impossible"* to identify analytically the Green's function of such plates.

where α is the strength of the Green's function and is calculated by means of a generalized inverse approach assuming that the measured field W is equal to the virtual field $\tilde{W}$:

$$\alpha(\omega) = \left(\mathcal{G}^{\mathrm{T}}\mathcal{G}\right)^{-1}\mathcal{G}^{\mathrm{T}}\mathcal{W}, \tag{6}$$

where the right hand side of Eq. (6) is evaluated for each frequency ω separately, and where $\mathcal{W}$ and $\mathcal{G}$ are vectors containing $W(x_p, y_q, \omega)$ and $G_\infty(x_p, y_q, \omega)$, respectively, for each frequency ω being considered. The superscript $^{\mathrm{T}}$ indicates the transpose of the vector. The reconstruction error between the measured $\mathcal{W}$ and projected $\tilde{\mathcal{W}}$ vibration fields is then given by:

$$e(\omega) = \frac{\|\mathcal{W} - \tilde{\mathcal{W}}\|^2}{\|\mathcal{W}\|^2}, \tag{7}$$

where $\|...\|$ denotes the Euclidean norm of a matrix.

The fitting procedure consists in calculating the error (Eq. (7)) at each frequency for different projected field, varying the parameters of the Green's function. These parameters correspond to the two flexural rigidities D'_{11}, D'_{22} and the orthotropy angle θ', assuming that the surface mass ρh of the plate is known. The values of these parameters that minimize the error are considered as the dynamic material characteristics of the plate. For structures with damping, in general the flexural rigidities are complex. In this study, we will essentially focus on the identification of the real part of these parameters, thus ignoring dissipation terms.

3 Reference characterisation techniques and analytical model

In order to validate the proposed Hankel fitting approach developed in section 2, we will use the IWC [1] (Inhomogeneous Wave Correlation) characterisation technique as well as an analytical model of multilayer systems as references and compare their results. This section briefly describes these two methods.

3.1 IWC method

The IWC method considers the same measured transverse vibration field $W(x_p, y_q, \omega)$. The projected field used in this correlation method corresponds to an inhomogeneous wave ϕ defined by a propagation angle θ and a wavenumber k:

$$\phi_{k,\theta}(x_p, y_q) = e^{-\mathrm{j}k(x_p\cos(\theta)+y_q\sin(\theta))}. \tag{8}$$

The correlation coefficient between the inhomogeneous wave and the measured

field is defined by:

$$\mathrm{IWC}(k,\theta) = \frac{\left|\sum_p \sum_q W(x_p, y_q, \omega)\phi^*_{k,\theta}(x_p, y_q)\right|}{\sqrt{\sum_p \sum_q |W(x_p, y_q)|^2 . \sum_p \sum_q |\phi_{k,\theta}(x_p, y_q)|^2}}, \tag{9}$$

where the superscript $*$ denotes the complex conjugate. As mention in the previous section, this study is focused on the identification of the elastic parameters of the structure. Hence, the wavenumber k is supposed to be real. At each angular frequency ω, the coefficient (9) is calculated for different values of the propagating parameters (k, θ). For a given θ and ω, the value of k that maximizes the IWC coefficient is considered as the flexural wavenumber of the structure $k_{\mathrm{f}}(\theta, \omega)$.

In a similar way as the Hankel fitting approach, we assume that the measured structure behaves as a thin plate of Love-Kirchhoff. This hypothesis implies that the flexural wavenumber $k_{\mathrm{f}}(\theta, \omega)$, identified by the IWC method, is a solution of the dispersion relation of the equivalent thin plate. This relation is defined as function of ω and θ by:

$$\mathcal{D}_i = \frac{\rho h \omega^2}{k^4_{\mathrm{f}}(\theta, \omega)}, \tag{10}$$

where $\mathcal{D}_i$ depends on the nature of the equivalent plate. Three different equivalent plate characteristics are studied in this section, i.e.

a) *Anisotropic plate characteristics* ($i = 1$). In this case, the dispersion relation is defined by five flexural rigidities D. The coefficient $\mathcal{D}_1$ can be written as:

$$\mathcal{D}_1 = D_{11}c^4_\theta + D_{22}s^4_\theta + D_{12}c^2_\theta s^2_\theta + D_{16}c^3_\theta s_\theta + D_{26}c_\theta s^3_\theta, \tag{11}$$

with $c_\theta = \cos(\theta)$ and $s_\theta = \sin(\theta)$.

b) *Orthotropic plate characteristics* ($i = 2$). In this case, the dispersion relation is defined by three flexural rigidities D' and the orthotropy angle θ'. The coefficient $\mathcal{D}_2$ can be written as:

$$\mathcal{D}_2 = D'_{11}c^4_{\theta-\theta'} + D'_{22}s^4_{\theta-\theta'} + D'_{12}c^2_{\theta-\theta'}s^2_{\theta-\theta'}, \tag{12}$$

with $c_{\theta-\theta'} = \cos(\theta - \theta')$ and $s_{\theta-\theta'} = \sin(\theta - \theta')$.

c) *Elliptical orthotropic plate characteristics* ($i = 3$). In this final case, the previous D' coefficients are related to each other by the relation $D'_{12} = 2\sqrt{D'_{11}D'_{22}}$. The coefficient $\mathcal{D}_3$ is then written as:

$$\mathcal{D}_3 = \left(\sqrt{D'_{11}}c^2_{\theta-\theta'} + \sqrt{D'_{22}}s^2_{\theta-\theta'}\right)^2. \tag{13}$$

For a given angular frequency ω, the equivalent characteristics, written as $\mathcal{X}_i$, can be identified for each case i using the following minimization problem:

$$\mathcal{X}_i = \underset{\mathcal{X}_i}{\mathrm{argmin}} \left(\sum_\theta \left| \mathcal{D}_i - \frac{\rho h \omega^2}{k^4_{\mathrm{f}}(\theta, \omega)} \right|^2 \right), \tag{14}$$

where

$$\mathcal{X}_1 = \Big\{D_{11}, D_{22}, D_{12}, D_{16}, D_{26}\Big\},$$
$$\mathcal{X}_2 = \Big\{D'_{11}, D'_{22}, D'_{12}, \theta'\Big\},$$
$$\mathcal{X}_3 = \Big\{D'_{11}, D'_{22}, \theta'\Big\}.$$

This minimization problem can be solved using the Nelder-Mead's method [18] which is based on a non-linear simplex algorithm. We can observe that the number of characterisation parameters decreases as soon as we add hypothesis on the nature of the equivalent plate (i.e. i increases).

3.2 Equivalent analytical model

The analytical model used in this paper was initially developed by Guyader and Lesueur [19] for orthotropic multilayers and has been extended to anisotropic structures by Loredo and Castel [20]. The behaviour of each layer is described by a Reissner-Mindlin's displacement field taking into account the flexural, membrane and shearing effects. The transverse displacement is supposed to be constant for all layers, neglecting the deformation through the thickness. An energetic methodology governed by Hamilton's principle is used to derive the equations of motion and the dispersion curves of the plate as function of the angular frequency ω and the direction θ.

In order to characterize the structure, the same equivalent methodology as mentioned in section 3.1 can be applied using the flexural wavenumber estimated by the model. Three different equivalent plate characteristics (anisotropic, orthotropic or elliptical orthotropic) have been assumed as well. Note that a similar equivalent methodology has already been studied with this analytical model for the anisotropic case on carbon fiber composite plates [21].

4 Experimental application

This section focuses on an experimental application of the proposed Hankel fitting approach presented in Section 2. This application deals with the characterisation of a honeycomb sandwich structure over a large frequency band. Comparisons with the IWC method and the analytical model presented in Section 3 are also given.

4.1 Protocol

The structure under test is composed of two aluminium skins separated with a Nomex honeycomb core. The thickness of each skin is 0.6 mm while the thickness of the core is 9 mm. The area of the plate is 0.73×0.52 m^2.

The plate is hung to a frame using elastics in order to tend toward free-free boundary conditions (see Fig. 2). A broadband chirp excitation is applied on the structure by means of a thin piezoelectric actuator (type EPZ-20MS64W from Ekulit) glued in the middle of the plate. The transverse displacement field of the structure is measured on a regular 2D mesh grid around the excitation by means of a 3D infrared scanning laser Doppler vibrometer (PSV 500 XTRA, Polytec). Note that the axes of this mesh (x, y) are parallel to the edges of the plate. A rope is threaded into holes placed in the edges of the plate to locally increase the damping at the edges of the structure. This procedure is used to attenuate the reflected waves and improve the performances of the IWC and Hankel fitting methods.

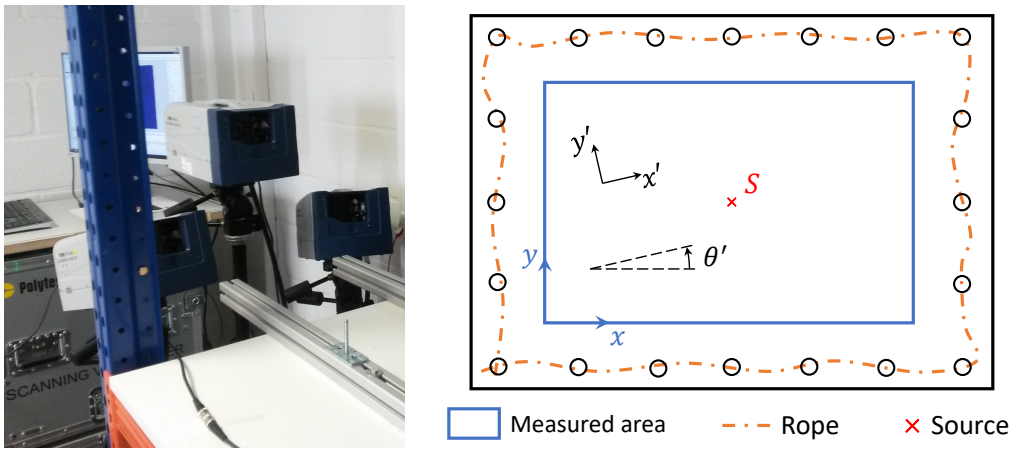

Fig. 2. Measurement set-up. Laser Doppler Vibrometer (left). Sketch of the measured honeycomb plate structure (right).

Two measurements have been performed in the frequency ranges 1–10 kHz and 10-50 kHz to reduce experimental noise levels due to high sample frequencies. Different configurations of mesh have been used for each measurement to obtain at least 3 points per wavelength at the maximum frequency (see Table 1).

4.2 Reconstruction error of the Hankel approach

In a first analysis, a 2D spatial Fourier Transform was applied to the measurement data to observe the flexural wavenumber in the k-space domain. Figure 3 presents this result at 18 kHz and 45 kHz. At 18 kHz, the non-circular shape of the maximum of level means that the flexural behaviour of the structure is orthotropic. This

	Measurement n°1	**Measurement n°2**
Frequency band	1 - 10 kHz	10 - 50 kHz
Sample frequency	25 kS/s	125 kS/s
Mesh	138×94 points	270×187 points
Spatial steps	$d_x = d_y \approx 4$ mm	$d_x = d_y \approx 2$ mm

Table 1
Characteristics of the measurements performed on the honeycomb sandwich plate by means of a Laser Doppler Vibrometer.

orthotropy is due to the honeycomb core and, based upon its shape, can be considered elliptical. We also observe that the axes of orthotropy (dashed blue lines in Figure 3) are not aligned with the axes of the measurement mesh (x, y). The orthotropy angle θ' (which is unknown) between the two coordinate system as well as the axes of orthotropy (x', y') are drawn in Figure 2. At 45 kHz, the shape of the maximum of level of the Fourier transform seems more circular meaning that the behaviour of the structure at higher frequencies tends to be isotropic.

Based on the previous observations, we can assume that the honeycomb sandwich can be described as an elliptical orthotropic plate. Thus, the hypothesis of the proposed Hankel fitting approach are well adapted to characterise the structure under test.

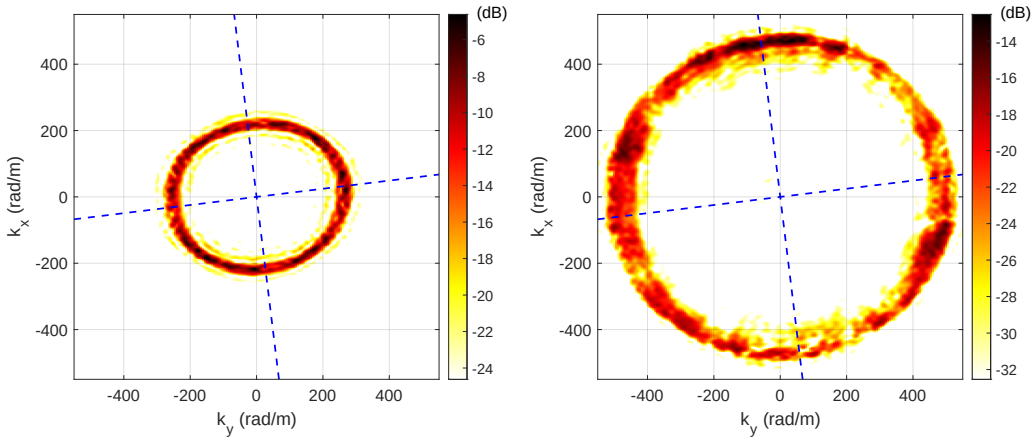

(a) $f = 18$ kHz (b) $f = 45$ kHz

Fig. 3. Spatial Fourier Transform applied on the measured transverse displacement field of the honeycomb structure at 18 kHz (a) and 45 kHz (b). Assumed orthotropy axes (blue dashed lines).

The proposed Hankel fitting approach has been applied to the measured data. Figure 4a presents the reconstruction error e (Eq. (7)) of the Hankel approach and the measured quadratic FRF as function of frequency. Both spectra contain the results of measurement 1 and 2. From 4.5 kHz up to 25 kHz, the reconstruction error is relatively low since the hypothesis of the method (i.e. omnidirectional source in free

field) are valid in this frequency range as can be seen in Figure 5b. Below 4.5 kHz, the modal behaviour of the structure involves a higher amount of error since the free field assumption is not respected (see Figure 5a). Above 25 kHz, the higher reconstruction error can be explained by the fact that the source is not omnidirectional (see Figure 5c). This non-omnidirectionality is caused by the fact that the natural wavelength of the structure is lower than the diameter of the piezoelectric actuator (20 mm). The small discontinuity of the error spectrum at 10 kHz can be explained by the fact that we use two different datasets.

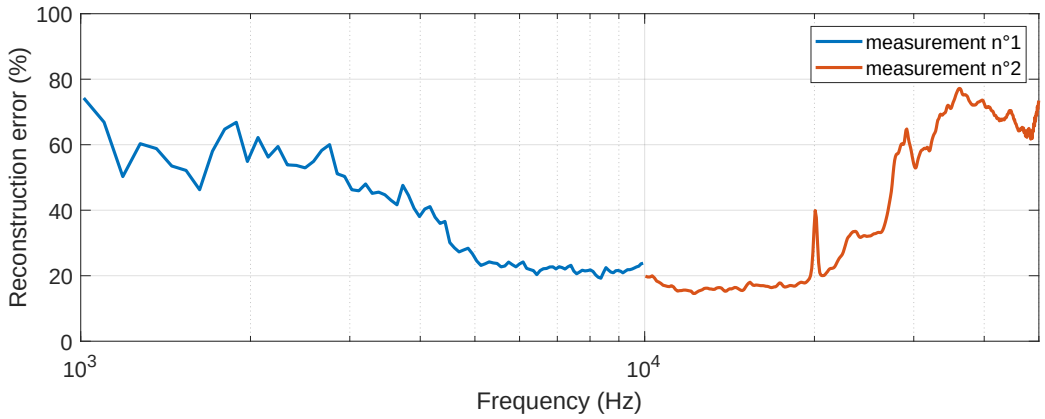

(a) Error spectrum

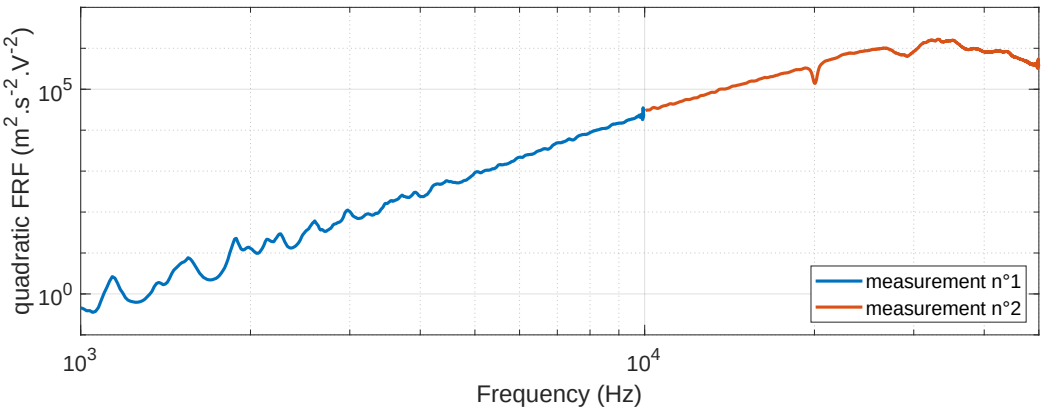

(b) Quadratic frequency response function

Fig. 4. Error spectrum (Eq. (7)) of the Hankel fitting approach (a) and measured quadratic frequency response function (b).

4.3 Characterisation of the structure

Figure 6 compares the angle of orthotropy identified by the Hankel approach and the IWC method (only for orthotropic and elliptical orthotropic plate characteristics) as function of frequency. Between 4.5 and 25 kHz, the results are approximately constant for all techniques and converge to an average value of $\theta' \approx -7.2°$. We notice that the IWC method gives noisier results than the Hankel fitting approach in this frequency band. Below 4.5 kHz and above 25 kHz, the inconsisten-

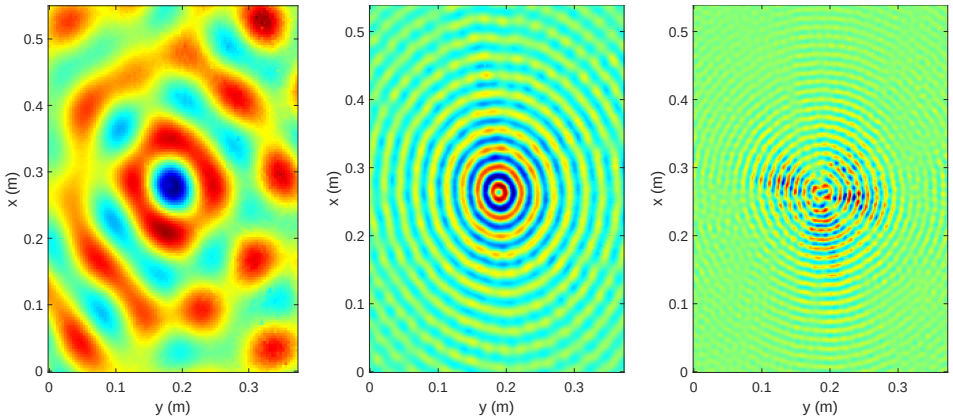

(a) $f = 4$ kHz (b) $f = 19$ kHz (c) $f = 45$ kHz

Fig. 5. Operational deflection shape measured at 4 (a), 19 (b) and 45 (c) kHz.

cies of the methods can be related to the observations made on the reconstruction error in section 4.2. We can also observed that the orthotropy angle identified by the IWC method is quite similar assuming elliptical or non-elliptical orthotropy.

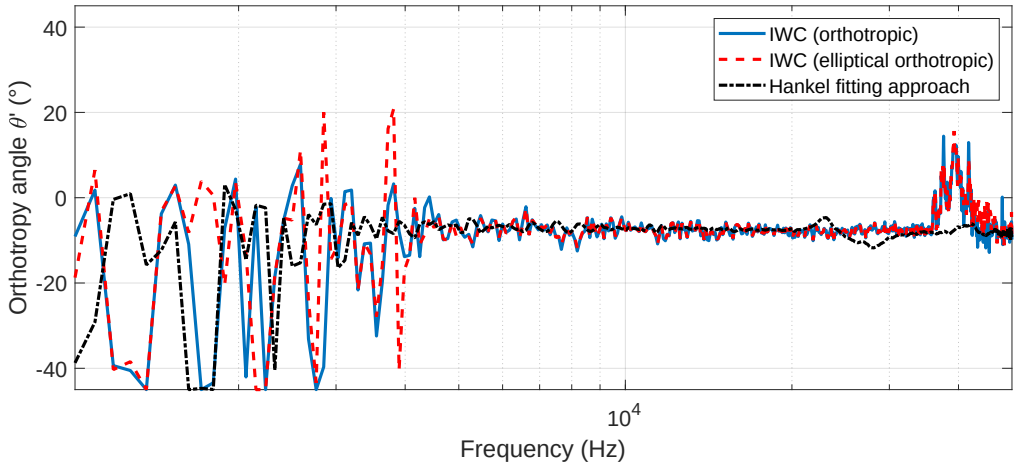

Fig. 6. Orthotropy angle identified by the Hankel fitting approach (black dot-dashed line) and the IWC method assuming orthotropic (blue line) and elliptical orthotropic (red dashed line) plate characteristics.

Figure 7 presents the flexural rigidities identified by the Hankel fitting approach for elliptical orthotropic plates as well as the IWC method using three different plate characteristics as defined in Section 3.1. The analytical model described in Section 3.2 is shown as well. Materials parameters of the layers used in the analytical model are summarized in Table 2. Classical parameters have been chosen for the aluminium skins. Concerning the honeycomb core, different simulations have been performed with the analytical model varying the parameters of this layer around values obtained from literature [22]. We selected the optimal parameters that minimize the differences between the flexural rigidities identified by the model and the IWC method (assuming anisotropic plate characteristic) on the whole frequency band. We noticed that the results of the model are essentially driven by the shear

modulus G_{xz} and G_{yz} as well as the mass density ρ of this layer. As a consequence, the other parameters of the core (Young's modulus E_x and E_y, shear modulus G_{xy} and Poisson's ratios ν_{xy} and ν_{yx}) have been assumed null. Finally, the value of the orthotropy angle of the honeycomb core has been chosen equal to $\theta' = -7.2°$ according to the experimental results described in Figure 6.

	Aluminium skins	**Nomex honeycomb core**
Thickness	$h = 0.6$ mm	$h = 9$ mm
Density	$\rho = 2700$ kg.m^{-3}	$\rho = 170$ kg.m^{-3}
Young's / shear modulus	$E = 70$ GPa	$G_{xz} = 50$ MPa; $G_{yz} = 115$ MPa
Poisson ratio	$\nu = 0.3$	-
Orthotropy angle	-	$\theta' = -7.2°$

Table 2
Mechanical parameters of the layers used in the analytical model.

Figure 7a shows the flexural rigidities identified by the IWC approach assuming full anisotropic plate characteristics. Five rigidities (D_{11}, D_{22}, D_{12}, D_{16} and D_{26}) are identified. Above 5 kHz the rigidities D_{11}, D_{22} and D_{12} correspond well with the rigidities predicted by the model. The rigidities D_{16} and D_{26} are noisier as compared to the estimates of D_{11}, D_{22} and D_{12} above 5 kHz. Below 5 kHz the identification is less good as a result of resonant behaviour and standing waves.

Figure 7b shows the flexural rigidities identified by the IWC approach assuming orthotropic plate characteristics. In this case, three rigidities are identified, i.e. D'_{11}, D'_{22} and D'_{12}. Again, above 5 kHz all three rigidities correspond well with the rigidities predicted by the model; no noticeable difference can be seen with respect to the IWC fitting results shown in Figure 7a.

Figure 7c shows the flexural rigidities identified by the IWC approach assuming elliptical orthotropic plate characteristics. In this case only two rigidities are identified, i.e. D'_{11} and D'_{22}. The estimated rigidities are smoother as compared to the previous cases, as a result of the fact that fewer parameters need to be estimated. The IWC fit results for an elliptical orthotropic plate characteristic correspond well with the model for frequencies above 4 kHz. This indicates that the elliptical orthotropic plate characteristic assumption seems to be a valid assumption in this case.

Figure 7d shows the flexural rigidities identified by the Hankel approach, also assuming an elliptical orthotropic plate characteristic. More consistent results are obtained with the analytical model as compared to the results of the IWC method shown in Figure 7c, especially in the frequency band 3-10 kHz.

Finally, the dynamic behaviour of the plate can be well described using the Hankel

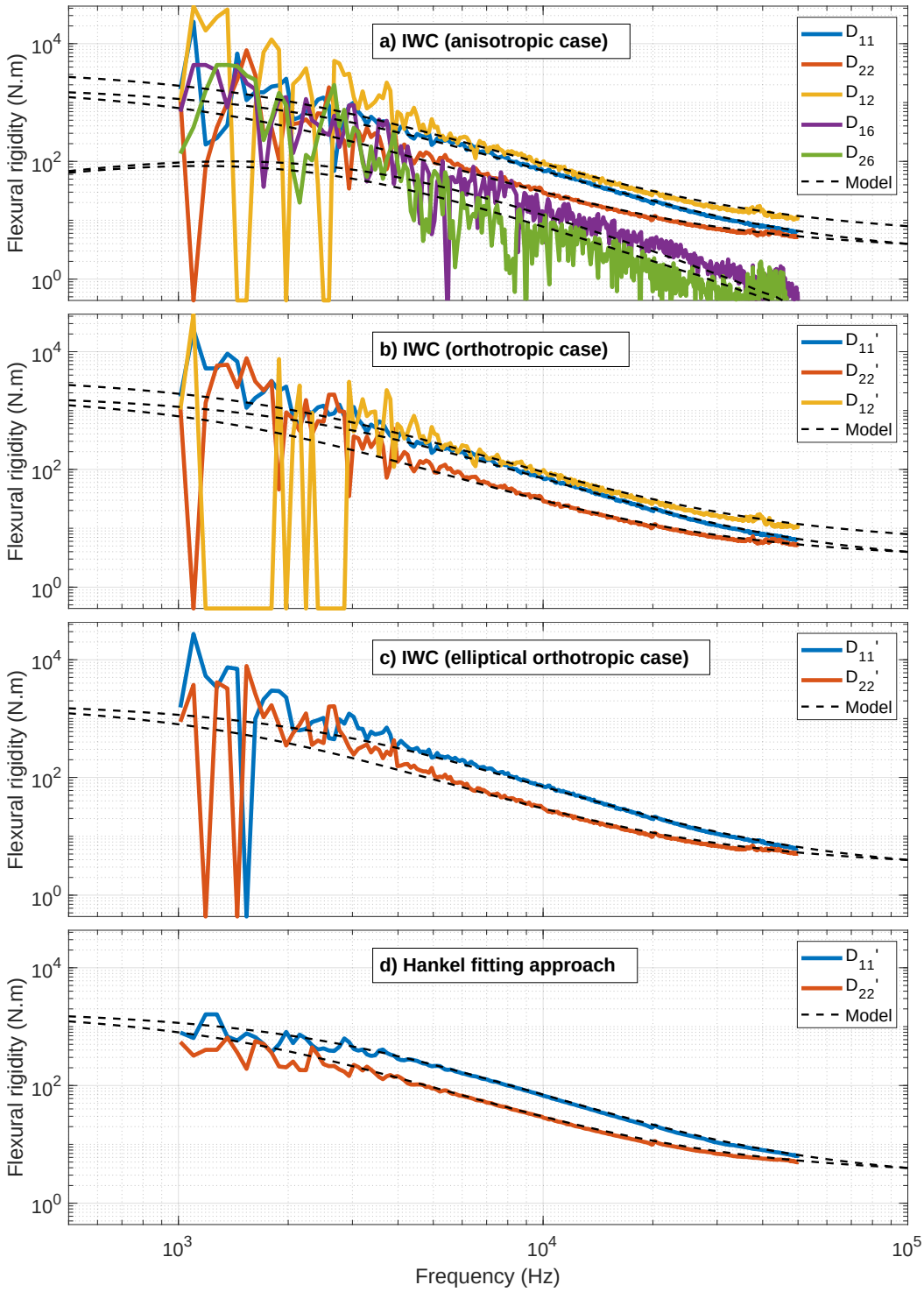

Fig. 7. Equivalent flexural rigidities identified with the IWC method for anisotropic (a), orthotropic (b), elliptical orthotropic (c) cases and Hankel fitting approach (d).

fitting approach or the IWC method assuming elliptical orthotropic plate characteristics. Figure 8 presents the ratio between the flexural rigidities D'_{11} and D'_{22} identified in Figures 7c and 7d. The observed dynamic behaviour is discussed below in

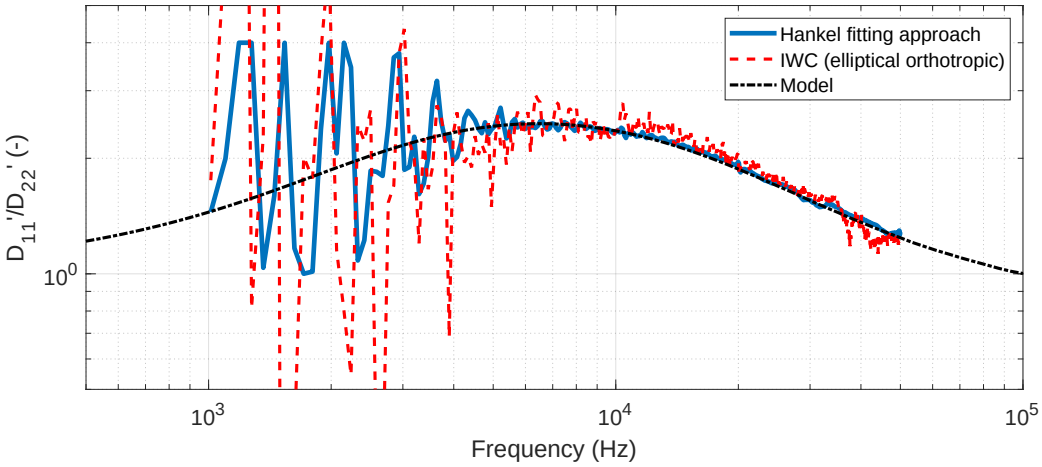

Fig. 8. Ratio between the flexural rigidities D'_{11} and D'_{22} identified by the Hankel fitting approach (blue line) and the IWC method assuming elliptical orthotropic plate characteristics (red dashed line) and estimated by the analytical model (black dot-dashed line).

three different frequency ranges. In the frequency range below 1 kHz, as estimated by the model, the behaviour of the structure is essentially controlled by the flexural motion of the skins. In this case, the ratio D'_{11}/D'_{22} tends to 1, meaning that the equivalent material properties are isotropic. In the mid frequency range between 1 and 50 kHz, the dynamic behaviour is governed by the shearing effect of the core. It involves a decrease of the equivalent flexural rigidities since the thin plate theory only considers the flexural motion of the structure. The equivalent material properties are anisotropic ($D'_{11}/D'_{22} \neq 1$). At higher frequencies, a decoupling effect of the layers is observed and the dynamic behaviour is controlled by the flexural motion of one skin. The equivalent material properties in this frequency range become, again, isotropic.

4.4 Influence of the excitation position on the Hankel fitting approach

The Hankel fitting approach requires the position (x_0, y_0) of the source exciting the plate. The performance of the method can be affected by the validity of this position. To illustrate this aspect, we applied the Hankel fitting approach on the measurements varying the excitation position in an area of 2×2 cm^2 around the assumed position. Figure 9 presents the error of the method (Eq. (7)) at 15 and 30 kHz as function of the deviation $(\Delta x_0, \Delta y_0)$ of the assumed point of excitation. For the current experimental application, a noticeable increase of the error can be avoided with a deviation smaller than 6 mm at 15 kHz and 3.5 mm at 30 kHz. From these observations, it can concluded that the allowable deviation decreases with increasing frequency and depends on the flexural wavelength of the structure, which is about 31 mm at 15 kHz and about 17 mm at 30 kHz according to the results of the IWC method (averaged in θ). It can be concluded from these results that the required precision for the source positioning is approximately a fifth of the

wavelength.

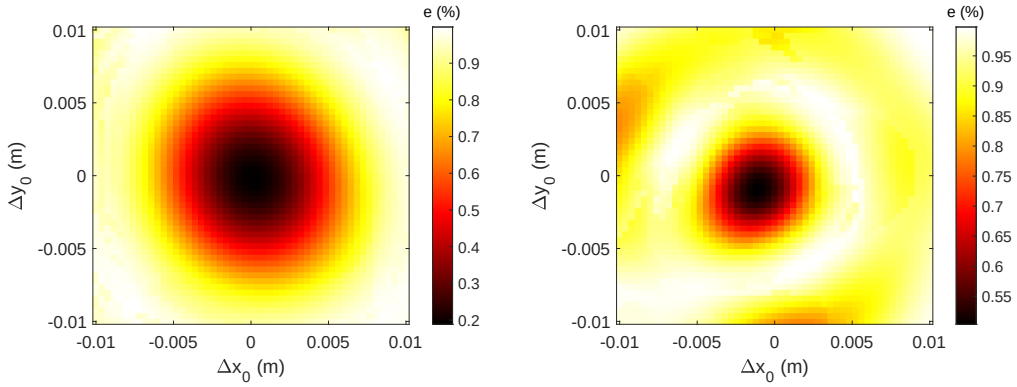

(a) $f = 15$ kHz (b) $f = 30$ kHz

Fig. 9. Error (Eq. (7)) of the Hankel fitting approach as function of the deviation $(\Delta x_0, \Delta y_0)$ of the assumed excitation position at 15 kHz (a) and 30 kHz (b).

4.5 Effects of the honeycomb cells

In the present work, it is assumed that the core of the honeycomb structure may be represented by means of an equivalent homogeneous orthotropic core structure. This assumption is validated experimentally through the spatial Fourier transform maps, exhibiting nice elliptical natural wavenumber curves (see Figure 3). Note that at the highest frequency considered in this study, the smallest natural wavelength $(2\pi/\max(k))$ is still larger than 10 mm, whilst the characteristic cell size is about 6 mm. However, the cell structure has some second order effects that are discussed hereafter.

A first effect is related to the drop in the quadratic velocity curve (see Figure 4b) observed at 20 kHz. This drop is associated to a peak in the fitting error (see Figure 4a), the operational deflection shape at this specific frequency is drawn in Figure 10. The high fitting error is due to a strong attenuation of the vibration level as a function of the distance to the source, much stronger than the assumed geometric attenuation in $1/\sqrt{r}$, caused by a distributed damping specifically acting at this frequency. 20 kHz corresponds to the first acoustic mode of the cell (half a wavelength in the thickness of the core), each cell thus acting as a (acoustically dominated) vibro-acoustic tuned-mass-damper, resonating at $f = 344/(2 * 0.009) \approx 20$ kHz. The distribution of these resonators logically generates a strong and distributed damping effect, explaining the observed attenuation. Such effect can be related to the singularity observed by Margerit et al [23] around 34 kHz on a similar honeycomb sandwich (of around 5 mm of thickness) for both real and imaginary parts of the identified complex wavenumbers [2] .

[2] Note that, in [23], the acoustic phenomenon $(c_0/(2h))$ coincides in frequency with the resonance of the cells (half-wavelength π/k around the cell size ($\approx$ 7 mm)

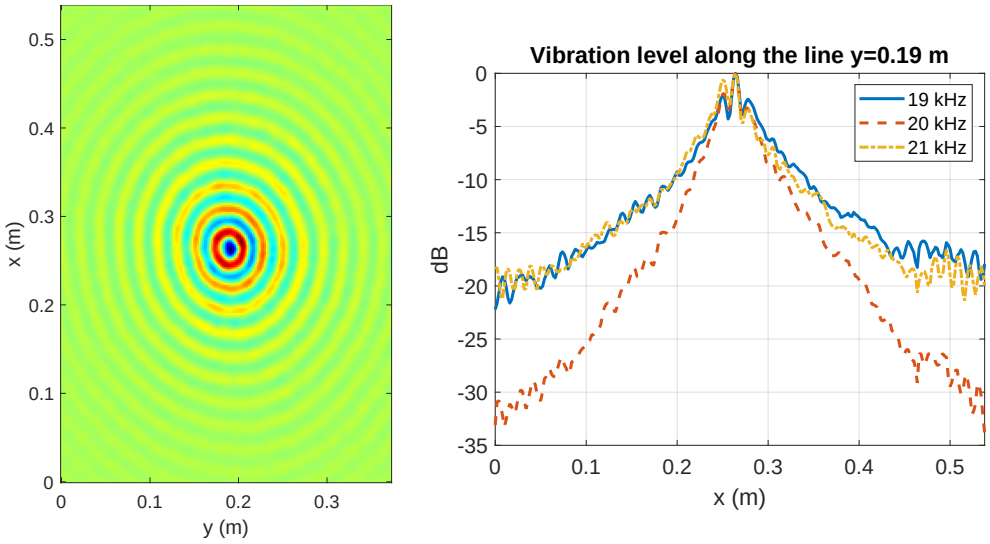

Fig. 10. Operational deflection shape measured at 20 kHz (left) and vibration level along the line $y = 0.19$ m (right).

A second effect can be observed at high wavenumbers. The cell structure has indeed a second order effect on the velocity field that can be interpreted as a spatial modulation of the vibration amplitude, at wavenumbers moduli and angles related to the geometry of the cell. This modulation in the space domain is clearly visible in the wavenumber domain as a replication of the natural wavenumber ellipse centred on specific points of the k-space (see Figure 11), these points can be related to the spatial periodicity and orientation of the honeycomb. The frequency evolution of the replications of the natural wavenumber is described in the following youtube video: `https://www.youtube.com/watch?v=Z0uhGErDx4M`, showing the measured velocity field and the K-space as function of frequency.

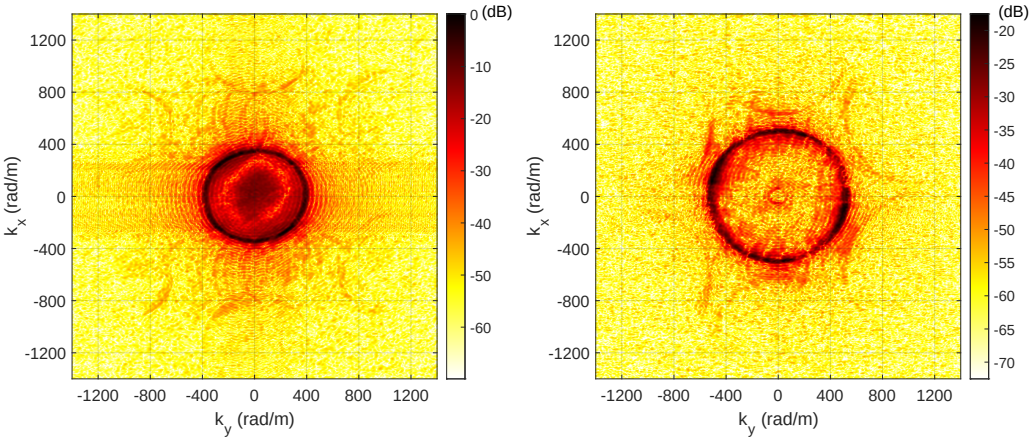

(a) $f = 30$ kHz (b) $f = 48$ kHz

Fig. 11. Spatial Fourier Transform applied on the measured transverse displacement field of the honeycomb structure at 30 kHz (a) and 48 kHz (b).

5 Conclusion

In this paper, the Hankel fitting approach is extended for the characterisation of elliptical orthotropic plates, using the equivalent thin plate theory. The Green's function used in the theory is adapted to handle structures with elliptical orthotropic stiffness properties. Three parameters, which correspond to the two flexural rigidities in the orthotropy axes and the main orthotropy angle, can be identified with the method. To validate the proposed Hankel fitting approach, experiments are performed on a honeycomb sandwich. The results of the method are compared with the estimations of the IWC method and an analytical model assuming three different plate characteristics (anisotropic, orthotropic and elliptical orthotropic). Assuming elliptical orthotropic plate characteristics, the Hankel approach shows more consistent results with the analytical model than the IWC method. Assuming full anisotropic material characteristics, estimating five rigidities, the IWC method gives noisier estimates, as a result of the fact that more parameters are estimated, which makes the method more sensitive to measurement noise.

A perspective of this study could be to extend the theory of the Hankel fitting approach for fully orthotropic or anisotropic plates using a numerical computation of the Green's function of such structures. Note that the computation time of the fitting procedure would be significant for orthotropic or anisotropic plates since the number of unknown characteristics increases in these cases. Another interesting research line could be to compare the proposed Hankel fitting approach with the recent extension of the CFAT approach for anisotropic plates [24].

Acknowledgments

This work was performed within the framework of the Labex CeLyA of Université de Lyon, operated by the French National Research Agency (ANR-10-LABX-0060/ ANR-11-IDEX-0007). Fonds voor Wetenschappelijk Onderzoek Vlaanderen (FWO grant 1148018N). J.S. and M.K. acknowledge funding through Fonds voor Wetenschappelijk Onderzoek Vlaanderen (FWO grant 1148018N).

References

[1] J. Berthaut, M. N. Ichchou, L. Jezequel, K-space identification of apparent structural behaviour, Journal of Sound and Vibration 280 (2005) 1125–1131.

[2] R. Cherif, J.-D. Chazot, N. Atalla, Damping loss factor estimation of two-dimensional orthotropic structures from a displacement field measurement, Journal of Sound and Vibration 356 (2015) 61 – 71.

[3] M. Ichchou, O. Bareille, J. Berthaut, Identification of effective sandwich structural properties via an inverse wave approach, Engineering Structures 30 (10) (2008) 2591 – 2604.

[4] M. Rak, M. Ichchou, J. Holnicki-Szulc, Identification of structural loss factor from spatially distributed measurements on beams with viscoelastic layer, Journal of Sound and Vibration 310 (4) (2008) 801 – 811.

[5] J. McDaniel, P. Dupont, L. Salvino, A wave approach to estimating frequency-dependent damping under transient loading, Journal of Sound and Vibration 231 (2) (2000) 433 – 449.

[6] J. Cuenca, F. Gautier, L. Simon, The image source method for calculating the vibrations of simply supported convex polygonal plates, Journal of Sound and Vibration 322 (4) (2009) 1048 – 1069.

[7] J. Cuenca, F. Gautier, L. Simon, Measurement of complex bending stiffness of a flat panel covered with a viscoelastic layer using the image source method, Vol. 31, Edinburgh, 2009.

[8] N. B. Roozen, Q. Leclère, K. Ege, Y. Gerges, Estimation of plate material properties by means of a complex wavenumber fit using hankel's functions and the image source method, Journal of Sound and Vibration 390 (2017) 257–271.

[9] C. Pézerat, J. Guyader, Identification of vibration sources, Applied Acoustics 61 (3) (2000) 309 – 324.

[10] Q. Leclère, C. Pézerat, Vibration source identification using corrected finite difference schemes, Journal of Sound and Vibration 331 (6) (2012) 1366–1377.

[11] F. Ablitzer, C. Pézerat, J. Génevaux, J. Bégué, Identification of stiffness and damping properties of plates by using the local equation of motion, Journal of Sound and Vibration 333 (9) (2014) 2454 – 2468.

[12] Q. Leclère, F. Ablitzer, C. Pézerat, Practical implementation of the corrected force analysis technique to identify the structural parameter and load distributions, Journal of Sound and Vibration 351 (2015) 106–118.

[13] F. Ablitzer, C. Pézerat, B. Lascoup, J. Brocail, Identification of the flexural stiffness parameters of an orthotropic plate from the local dynamic equilibrium without a priori knowledge of the principal directions, Journal of Sound and Vibration 404 (2017) 31 – 46.

[14] F. Pierron, M. Grédiac, The virtual fields method. Extracting constitutive mechanical parameters from full-field deformation measurements, Springer-Verlag, 2012.

[15] J. L. Guyader, C. Cacciolati, Viscoelastic properties of single layer plate material equivalent to multi-layer composites plate, Internoise (2007) 1558–1567.

[16] J. Berthaut, Contribution à l'identification large bande des structures anisotropes : Application aux tables d'harmonie des pianos, Ph.D. thesis, Ecole Centrale de Lyon (2004).

[17] J. F. Hamet, Propagating wave formulation of tire vibrations using the orthotropic plate model, in: InterNoise 2002, Michigan, United States, 2015.

[18] J. Lagarias, J. Reeds, M. Wright, P. Wright, Convergence properties of the nelder–mead simplex method in low dimensions, SIAM Journal on Optimization 9 (1998) 112–147.

[19] J. L. Guyader, C. Lesueur, Acoustic transmission through orthotropic multilayered plates, part 1: Plate vibration modes, Journal of Sound and Vibration 58 (1978) 51–68.

[20] A. Loredo, A. Castel, A multilayer anisotropic plate model with warping functions for the study of vibrations reformulated from Woodcock's work, Journal of Sound and Vibration 332 (2013) 102–125.

[21] F. Marchetti, K. Ege, Q. Leclère, N. B. Roozen, On the structural dynamics of laminated composite plates and sandwich structures; a new perspective on damping identification, Journal of Sound and Vibration 474 (2020) 115256.

[22] E. Nilsson, A. C. Nilsson, Prediction and measurement of some properties of sandwich structures with honeycomb and foam cores, Journal of Sound and Vibration 251 (2002) 409–430.

[23] P. Margerit, A. Lebée, J.-F. Caron, K. Ege, X. Boutillon, The high-resolution wavevector analysis for the characterization of the dynamic response of composite plates, Journal of Sound and Vibration 458 (2019) 177–196.

[24] F. Marchetti, K. Ege, Q. Leclère, Development of the corrected force analysis technique for laminated composite panels, Journal of Sound and Vibration (2020) 115692.

List of Figures

List of Tables